Synthesis of the bulky phosphanide $[P(Si^{i}Pr_3)_2]^-$ and its stabilisation of low-coordinate Group 12 complexes.

Olivia P. Churchill,[a],† Antonia Dase,[a],† Laurence J. Taylor,[a] Stephen P. Argent,[a] Nathan T. Coles,[a,b] Gavin S. Walker[c] and Deborah L. Kays[a,b],*

[a] School of Chemistry, University of Nottingham, University Park, Nottingham, NG7 2RD (UK)

[b] School of Chemistry, Cardiff University, Main Building, Park Place, Cardiff, CF10 3AT

[c] Advanced Materials Research Group, Faculty of Engineering, University of Nottingham, NG7 2GA (UK)

† These authors contributed equally to this manuscript.

E-mail: KaysD@cardiff.ac.uk

Abstract

Here, we report the first practical synthesis of the bulky phosphanide anion $[P(Si^{i}Pr_3)_2]^-$ in synthetically useful yields, and its complexation to Group 12 metals. The ligand is obtained as the sodium salt $(DME)NaP(Si^{i}Pr_3)_2$ **1** (DME = 1,2-dimethoxyethane) in 36% isolated yield and a single step from red phosphorus and sodium. This far exceeds previous yields for this ligand (*ca.* 9.8% overall yield over 3 steps), and we have thus applied **1** to the synthesis of the two coordinate complexes $M[P(Si^{i}Pr_3)_2]_2$ (M = Zn, Cd, Hg). These Group 12 complexes are all monomeric and with non-linear P–M–P angles [163.593(18)° to 170.086(16)°] in the solid state, with DFT calculations suggesting that this bending is due to the steric demands of the ligand. Multinuclear NMR spectroscopy revealed complex 2nd order splitting patterns due to strong PP' coupling. This work demonstrates that the synthesis of **1** is viable and provides a springboard for the synthesis of low-coordinate d-block complexes featuring this unusual bulky ligand.

Introduction

The use of sterically demanding ligands to enforce low-coordination geometries upon d- and f-block metal centres remains an area of interest for inorganic chemists.[1–5] Such complexes are typically highly reactive and thus capable of acting as a catalyst or activating small molecules.[3,6–15] These complexes can also display unusual physical properties, such as single molecule magnet (SMM) behaviour.[16–25] The use of amides as sterically demanding ligands dates to the 1960s, with the use of the $[N(SiMe_3)_2]^-$ ligand to isolate two-coordinate d-block complexes.[26–28] Since then, a wide array of bulky silylamide ligands have been developed and utilized, such as $[N(Dipp)(SiMe_3)]^-$.[14,29–35] More recently, the exceedingly bulky $[KN(Si^{i}Pr_3)_2]$ has been applied to the synthesis of linear f-block species, which display large magnetic anisotropy and have the potential for extremely high U_{eff} values (U_{eff} = barrier to magnetization,[36–38] as well as group 2 Lewis acidic cations.[39] Most recently, investigations of $(^{t}Bu_3Si)_2NH$ showed the amide to be resistant to deprotonation even by $^{n}BuLi/KO^{t}Bu$ superbase mixtures. However, coordination of $(^{t}Bu_3Si)_2N^-$ to Cs was achieved through the reaction with Cs^0/THP electride solution (THP = tetrahydropyran) and the resulting $(^{t}Bu_3Si)_2NCs$ complex was shown to undergo a metathesis reaction when reacted with LiI.[40]

https://doi.org/10.26434/chemrxiv-2024-f4lkp **ORCID:** https://orcid.org/0000-0002-4948-4267

While bulky silylamides are relatively well established, the corresponding phosphorus analogues have received considerably less attention. Studies with $[P(SiMe_3)_2]^-$ ligands afforded dimeric, rather than monomeric, structures due to the larger size of the P atom.[41–43] To the best of our knowledge, the only two-coordinate metal bis(silylphosphanido) complexes to date are $M[P(SiPh_3)_2]_2$ (M = Zn, Cd, Hg), prepared by Matchett *et al.*[44] Here, the higher steric demands of the $-SiPh_3$ group offset the larger P atom, allowing for isolation of monomeric species. Thus, we propose that the phosphorus analogue of the above-discussed $[N(Si^iPr_3)_2]^-$ ligand is of considerable interest due to its steric bulk, which should allow the isolation of monomeric complexes. While the $[P(Si^iPr_3)_2]^-$ ligand is known, it has scarcely been studied due to difficulties in its preparation. Westerhausen *et al.* prepared the Li salt $[(THF)LiP(Si^iPr_3)_2]_2$ by first reacting ^nBuLi with PH_3 in the presence of DME (DME = 1,2-dimethoxyethane) to obtain $(DME)LiPH_2$ in an 82–91% yield.[45,46] This was then reacted $^iPr_3SiCl$ to afford $P(Si^iPr_3)_3$ (64%) and $(^iPr_3Si)_2PH$ (13%).[47] Further reaction of the minor product $(^iPr_3Si)_2PH$ with ^nBuLi in THF afforded $[(THF)LiP(Si^iPr_3)_2]_2$ in 83% yield,[48] giving an overall yield from PH_3 of at most 9.8%. Given the difficult and low-yielding synthesis, $[(THF)LiP(Si^iPr_3)_2]_2$ was used to prepare only one complex, $[(THF)_4Li][(^iPr_3Si)_2PW(CO)_5]$.[48] As such, the potential of this ligand is largely unexplored.

Herein, we present a much-improved synthesis of an alkali metal complex of this ligand, the Na^+ salt $(DME)NaP(Si^iPr_3)_2$ (**1**), which has been obtained in a 36% isolated yield and in a single step. This has allowed us to prepare the family of Group 12 complexes $M[P(Si^iPr_3)_2]_2$ (M = Zn (**2**), Cd (**3**), Hg (**4**)), demonstrating the synthetic utility of this ligand precursor in transmetallation reactions.

Results and discussion

$(DME)NaP(Si^iPr_3)_2$ **1**

To obtain a more direct route to the $[P(Si^iPr_3)_2]^-$ anion than previously reported,[48] we looked to the synthesis of $P(Si^iPr_3)_3$ published by von Hänisch. Here, red phosphorus was reacted with NaK in refluxing DME to generate $(Na/K)_3P$, which was subsequently reacted with $^iPr_3SiCl$.[49] Since $P(SiMe_3)_3$ can be converted to $(Me_3Si)_2PH$ by hydrolysis or methanolysis,[50,51] we postulated that it could be possible to obtain $(^iPr_3Si)_2PH$ in a similar manner. However, the use of highly pyrophoric NaK alloy was a safety concern. To mitigate this, we instead used Na with 10 mol% naphthalene as an electron transfer agent.[52] This method has been used previously to generate Na_3P *in situ*,[53,54] for the preparation of tris(trimethylsilyl)phosphine, $P(SiMe_3)_3$.[55]

In our initial testing, we found that it was necessary to reflux the Na/naphthalene and red P for 24 hours in DME, otherwise the resultant product contained significant amounts of unreacted $^iPr_3SiCl$ and $(^iPr_3Si)_2$. This is believed to occur due to incomplete formation of Na_3P and the presence of unreacted Na. When monitoring the reaction by $^{31}P\{^1H\}$ NMR spectroscopy, we found that a mixture of P containing species were formed, including $(^iPr_3Si)_3P$ and $(^iPr_3Si)_2PH$, which were identified by comparison with the literature.[56] Another significant ^{31}P NMR signal was observed at −378 ppm (compound **1**). By removing the DME *in vacuo*, then extracting the resulting residue in hexane or toluene, it was possible to precipitate **1** from the reaction mixture as a white pyrophoric solid, while $P(Si^iPr_3)_3$, $(^iPr_3Si)_2PH$, and other P-containing by-products remained in solution. ^1H, $^{13}C\{^1H\}$, ^{31}P, and $^{31}P\{^1H\}$ NMR spectroscopy of **1** suggested the complex contained $-P(Si^iPr_3)_2$ and DME moieties in a 1:1 ratio (see Supporting Information Figures S2 and S3). While it was not possible to obtain crystals of **1** suitable for single crystal X-ray diffraction studies, crystals of $[(THF)NaP(Si^iPr_3)_2]_2$ (**1a**) were obtained when a reaction mixture containing **1** was dissolved in C_6D_6 and THF (Figure 1) and left at room temperature for four weeks. Based on this structure and the NMR spectroscopic data, we propose that

1 corresponds to (DME)NaP(Si^{i}Pr$_3$)$_2$. Due to the very high sensitivity of **1,** it was not possible to obtain high resolution mass spectrometric data on this compound.

Given that our aim had been to convert P(Si^{i}Pr$_3$)$_3$ to the [P(Si^{i}Pr$_3$)$_2$]$^-$ anion *via* a multi-step process, the observation of **1** was quite exciting. Here, we were directly forming a phosphanide anion in a single step and purifying it by precipitation and filtration. Thus, we focused on optimising the synthesis to maximise the yield of **1**, rather than P(Si^{i}Pr$_3$)$_3$. This led to the development of the methodology shown in **Error! Reference source not found.**. Na and 10 mol% naphthalene were refluxed in DME for 24 h ours, after which ^{i}Pr$_3$SiCl was added and the reaction heated for a further 24 hours. After filtration to remove insoluble impurities, the DME was removed *in vacuo* and the resulting oil was extracted into toluene. This precipitated **1**, which was isolated by filtration in 36% yield and sufficient purity for further synthesis. The crude reaction mixture showed the formation of **1**, (^{i}Pr$_3$Si)$_2$PH and P(Si^{i}Pr$_3$)$_3$ in an approximate 1:0.28:0.08 ratio (see Supporting Information Figure S6). (^{i}Pr$_3$Si)$_2$PH has been previously shown to be readily converted to [(THF)LiP(Si^{i}Pr$_3$)$_2$]$_2$,[48] which can also be used in transmetallation reactions, it is suggested that isolation of this by-product would further increase the yield of usable phosphanide precursors from this reaction. Note that, concurrent with our reported work, the Mills group has developed a similar (albeit lower yielding) synthesis of **1**.[57]

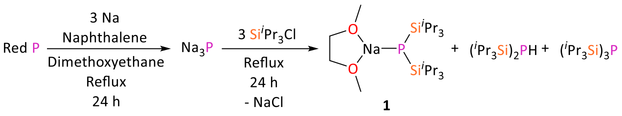

Scheme 1. Optimised synthesis of (DME)NaP(Si^{i}Pr$_3$)$_2$ (**1**).

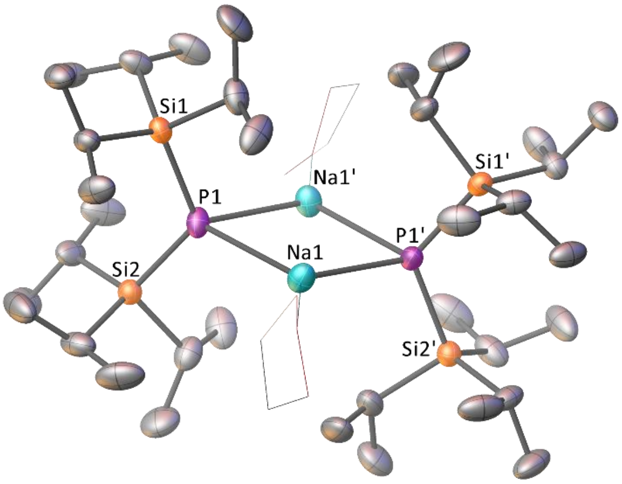

Figure 1. Single crystal XRD structure of [(THF)NaP(Si^{i}Pr$_3$)$_2$]$_2$ **1a**. Coordinated THF represented as a wireframe, minor disorder components and hydrogen atoms omitted for clarity. Thermal ellipsoids are set to 50% probability. Atoms marked with ' are obtained using the following symmetry operation, $1-x, +y, \frac{1}{2}-z$. Selected bond lengths (Å) and angles (°): Na1–P1 2.8039(11), Na1–P1' 2.806(1), Na–O1A 2.200(6), Na–O1B 2.203(6), Na–O1C 2.309(3), Na1···Na1' 3.4586(18), P1–Si1 2.2207(8), P1–Si2 2.2163(7), P1–Na1–P1' 103.84(3) Na1–P1–Na1' 76.15(3).

Group 12 complexes **2–4**

The two-coordinate Group 12 complexes **2**–**4** were prepared by the metathesis reaction of **1** with the appropriate metal halide (ZnCl$_2$, CdI$_2$, HgBr$_2$) in diethyl ether (Scheme 2). The resulting complexes were isolated as white crystalline solids in moderate to good yields (40–57%) after extraction and recrystallisation from *n*-hexane. For the formation of **3**, it was necessary to use CdI_2, as reactions between **1** and $CdCl_2$ in diethyl ether led to the precipitation of Cd(0). Complexes **2**–**4** are air and moisture sensitive and were characterized by single crystal X-ray diffraction and multinuclear NMR spectroscopy. Complex **2** was also characterized by HRMS and CHN microanalysis; the high toxicity of complexes **3** and **4** precluded their analysis by these methods.

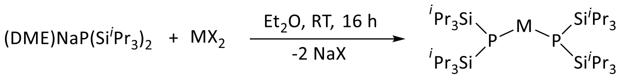

1

2: M = Zn
3: M = Cd
4: M = Hg

Scheme 2: Synthesis of Group 12 bis(silylphosphanido) complexes **2**–**4**. MX_2 = $ZnCl_2$, CdI_2, $HgBr_2$.

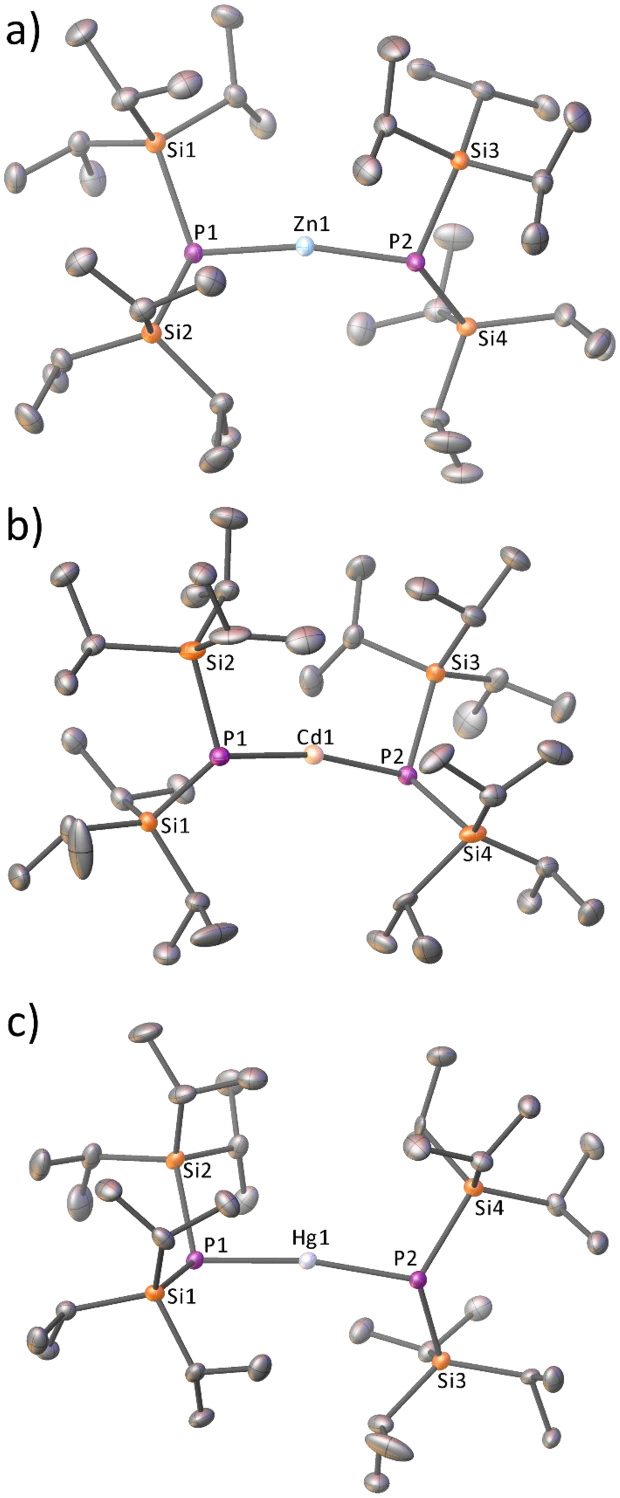

Figure 2: View of the single crystal X-ray diffraction studies of a) 2, b) 3 and c) 4. Hydrogen atoms and minor disorder components if 3 and 4 omitted for clarity. Thermal ellipsoids shown at 50% probability.

Table 1. Selected bond lengths (Å) and angles (°) for $M[P(Si^iPr_3)_2]_2$ (M = Zn (**2**), Cd (**3**), Hg (**4**)). Complexes **2**, **3**, and **4** were crystallised from *n*-hexane. **2a** is a polymorph of **2** crystallised from diethyl ether.

	2	**2a**	**3**	**4**
M1–P1	2.2291(3)	2.2309(4)	2.4213(7)	2.3946(5)
M1–P2	2.2234(4)	2.2562(4)	2.4216(7)	2.3930(5)
P1–Si1	2.2532(4)	2.2629(4)	2.2571(7)	2.2614(7)
P1–Si2	2.2537(4)	2.2550(5)	2.2487(7)	2.2657(8)
P2–Si3	2.2456(4)	2.2598(5)	2.2557(8)	2.2644(7)
P2–Si4	2.2479(4)	2.2527(4)	2.2570(6)	2.2541(8)
P1–M1–P2	168.747(12)	163.593(18)	169.215(19)	170.086(16)
∑° around P1	334.141(18)	337.05(13)	330.52(3)	325.73(3)
∑° around P2	339.755(17)	322.26(13)	324.87(3)	331.16(3)

Crystals of **2**–**4** suitable for single crystal X-ray diffraction were obtained from storage of saturated *n*-hexane solutions at −30 °C (Figure 2). A polymorph structure of **2** (**2a**) was also obtained by slow evaporation from diethyl ether (Figure S1. **2** and **2a** crystallise in the same space group ($P\bar{1}$) but with a differing unit cell (Table S1) and with significantly different P1–Zn1–P2 angles [168.747(12)° *vs* 163.593(18)°]. All structures show **2**–**4** to be monomeric and two-coordinate in the solid state. The M1–P1 and M1–P2 bond lengths (**Error! Reference source not found.**) are similar to those seen in the t erminal silyl phosphanido groups in$[M(P(SiMe_3)_2\{\mu_2\text{-}P(SiMe_3)_2\}]_2$ (Zn–P_t 2.295(1) Å, Cd–P_t 2.459(1) Å and Hg–P_t 2.402(1) Å).[42] The P–Si bond lengths differ slightly between complexes [2.2479(4)–2.2657(8) Å, Table 1] but are consistent with P–Si single bonds, with little evidence of P–Si double bond character [typical P=Si distances 2.062(1)-2.158(2) Å].[58] The sum of the angles around each phosphorus centre (Σ°, Table 1) is also consistent with an sp^3 hybridized P atom (*i.e.* no P=Si bond character). All of the complexes exhibit a P–M–P unit, with this angle increasing from Zn > Cd > Hg (Table 1).

Closed-shell, two-coordinate metal complexes are frequently linear,[59–68] although non-linear species are known.[66,69–71] Given that the only previous Group 12 bis(silylphosphanido) complex to be structurally characterized ($Cd[P(SiPh_3)_2]_2$) was linear,[44] DFT calculations were used to probe the reasons for the deviation from linearity for **2**–**4** in the solid state. Geometry optimizations were performed on **2**–**4** (PBE0/SARC-ZORA-TZVP for Cd and Hg, PBE0/ZORA-def2-TZVP for all other atoms).[72–79] The optimized structures were in good agreement with those determined experimentally, and in all cases reproduced the non-linear P–M–P (M = Zn, Cd, Hg) bond angles (Table S2). Models of **2**–**4** were also optimized with a 180° P–M–P bond angle restraint, affording linear models (**2'**, **3'**, **4'**). These linear models were found to be significantly *less* thermodynamically stable than the bent structures (ΔG = 13.3 kcal mol^{-1} for Zn; 10.7 kcal mol^{-1} for Cd; 8.9 kcal mol^{-1} for Hg). The linear structures show significant distortion about the P atoms, with asymmetry in the M–P–Si angles (Figure S31, Table S2). By contrast, the M–P–Si groups in the non-linear optimized structures were more symmetric (Figure S32, Table S2). This suggests that the bent P–M–P bond angles are a consequence of the steric demands of the $[P(Si^iPr_3)_2]^-$ ligands. To fit these ligands around the metal, it is necessary to distort at *either* the metal centre *or* the P atoms, with the distortion at the metal being more favourable. The solid state structure of $Cd[P(SiPh_3)_2]_2$ shows relatively symmetric Cd–P–Si angles (100.9(2)°, 98.2(1)°) and a linear P–Cd–P angle,[44] suggesting that a smaller ligand removes the need for distortion. Geometry optimization (without restraints) of the less sterically demanding $Cd[P(SiMe_3)_2]_2$, starting from linear and non-linear geometries, afforded both linear (P–Cd–P = 179.9°) and near-linear (P–Cd–P = 177.5°) molecules. These two geometries showed near-identical energies (ΔG = 0.1 kcal mol^{-1}), suggesting that there is little energetic difference between these two coordination environments for the less sterically demanding $[P(SiMe_3)_2]^-$ ligand.

NMR spectroscopic analysis

The $^{13}C\{^1H\}$ NMR spectra of **2**–**4** (Figure 3) and the ^{29}Si NMR spectrum of **4** (Figure 4) show evidence of second order effects due to strong virtual coupling between the ^{31}P nuclei ($^2J_{PP'}$). Similar effects have been reported in the literature for analogous phosphorus-carbon ABX and AA'X systems.[80–82] Despite the different appearances of the $^{13}C\{^1H\}$ NMR signals, the $^2J_{CP}$ and $^3J_{CP}$ coupling constants are similar across the series [$^2J_{CP}$ = 10.7 Hz (**2**), 10.3 Hz (**3**), 10.2 Hz (**4**); $^3J_{CP}$ = 3.6 Hz (**1**) 3.7 Hz (**2**), 3.5 Hz (**4**)]. This indicates that the differences between **2**–**4** are likely caused by the changing magnitude of $^2J_{PP'}$ across the series.

While the ^{29}Si NMR spectra of **2** and **3** show apparent doublets, that of **4** is more complex, consistent with an AA'X spin system with virtual coupling. This spectrum was well simulated with parameters of $^1J_{SiP}$ = 50.6 Hz, $^3J_{SiP'}$ = 0.0 Hz, $^2J_{PP'}$ = 19.0 Hz (Figure 4). This $^2J_{PP'}$ coupling of 19.0 Hz was also used to successfully simulate the $^{13}C\{^1H\}$ NMR signals of **4** (see Supporting Information Figures S25 and S26), further supporting this value for $^2J_{PP'}$.

Also of note are the ^{29}Si satellites in the $^{31}P\{^1H\}$ NMR spectra of **2**–**4**. While **2** and **4** show apparent ^{29}Si satellites, the measured coupling from these satellite peaks does not match that found in the ^{29}Si NMR spectra. This is likely due to the presence of one spin-active ^{29}Si nucleus causing the two ^{31}P nuclei to become magnetically inequivalent, such that the satellite signal is not a simple doublet. For **3**, the measured $^2J_{SiP}$ from the satellites does match the ^{29}Si NMR spectrum, suggesting that the two P atoms are (closer to) magnetically equivalent in **3**. The $^{31}P\{^1H\}$ NMR signal for **4** (δ_P = −209 ppm) occurs significantly downfield of the signals for **2** or **3** (δ_P = −288 and −284 ppm, respectively), which is consistent with previously published Group 12 bis(silylphosphanido) complexes.[44] The ^{113}Cd and ^{199}Hg NMR spectra of **3** and **4** both appear as triplets, with large couplings to phosphorus ($^1J_{CdP}$ = 350 Hz, $^1J_{HgP}$ = 408 Hz).

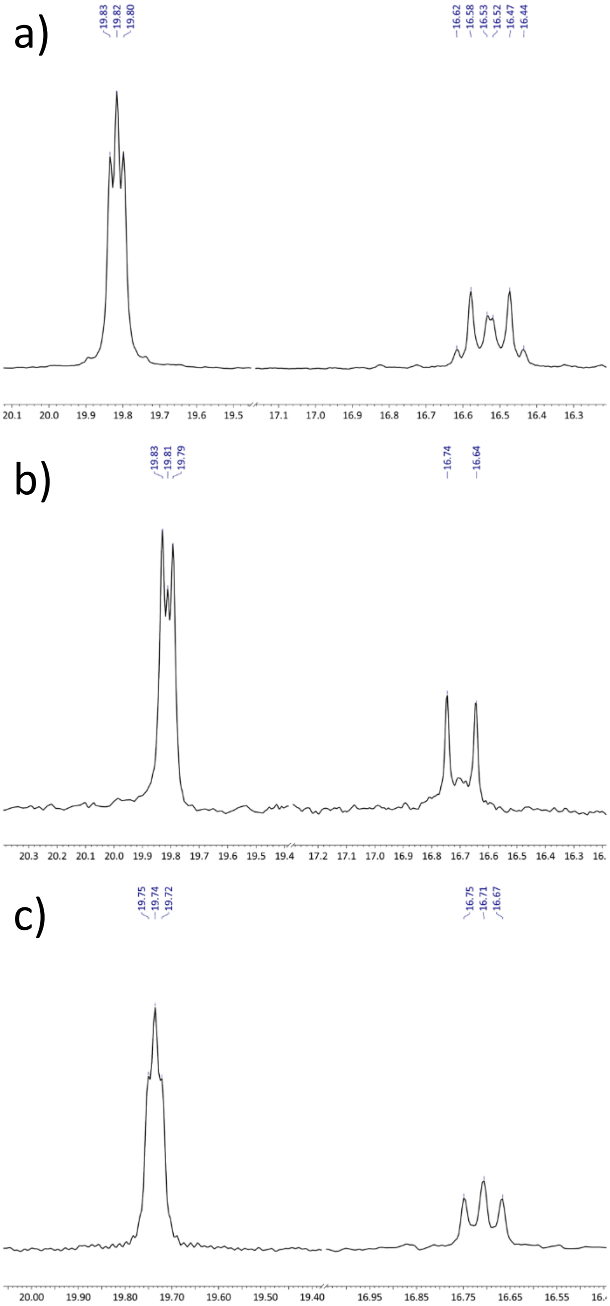

Figure 3: $^{13}C\{^{1}H\}$ NMR spectra of a) **2**, b) **3**, and c) **4** showing the extent of virtual coupling.

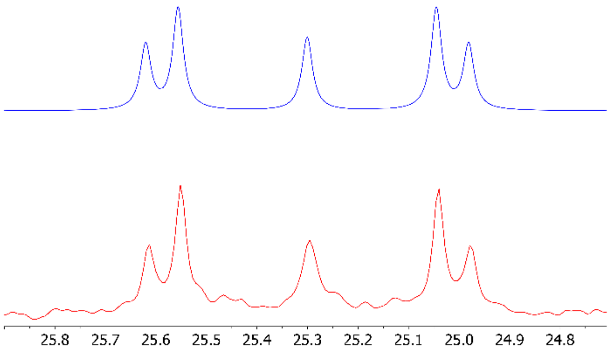

Figure 4: The experimental (red) and simulated (blue) ^{29}Si NMR spectrum of **4**, modelled using the parameters $^1J_{SiP}$ = 50.6 Hz, $^3J_{SiP'}$ = 0.0 Hz and $^2J_{PP'}$ = 19.0 Hz.

Conclusions

We present the first one-step synthesis of a source of the phosphanide anion $[P(Si^iPr_3)_2]^-$, in the form of $(DME)NaP(Si^iPr_3)_2$ (**1**). Complex **1** was obtained in 36% isolated yield, far higher than the previously reported Li phosphanide $[(THF)LiP(Si^iPr_3)_2]_2$, thereby offering a significantly improved route to the practical use of this ligand in synthesis. $[(THF)NaP(Si^iPr_3)_2]$, **1a** obtained from solvent exchange of **1** in THF, was characterized by single crystal X-ray diffraction. With this synthetically useful methodology to **1**, we were able to complex this sterically demanding phosphanide ligand to Zn, Cd, and Hg, affording the novel two-coordinate complexes **2**–**4**. Single crystal X-ray diffraction revealed that complexes **2**–**4** all show significant deviations from linearity in the solid state, with DFT calculations suggesting this is due to the steric demands of the ligand. ^{13}C{^{1}H} and ^{29}Si{^{1}H} NMR spectroscopy of these ligands revealed strong second-order effects, suggesting the presence of virtual coupling between the two ^{31}P nuclei in these complexes. These studies show that $[P(Si^iPr_3)_2]^-$ is now an accessible bulky, monodentate, monoanionic ligand.

Acknowledgements

We acknowledge the EPSRC [grant number EP/R004064/1; grant number EP/S023909/1]; the Leverhulme Trust [grant number RPG-2021-183] and the University of Nottingham for financial support of this research. We thank Prof. David Mills and co-workers at the Department of Chemistry, University of Manchester, for invaluable chemical discussions regarding the synthesis of the $[P(Si^iPr_3)_2]^-$ complexes. We also thank the University of Nottingham Analytical Services Team for mass spectrometry, CHN microanalysis, and NMR spectroscopy measurements. We thank Dr Kevin Butler and Dr Huw Williams at the University of Nottingham for advice on simulating NMR spectra. We are also grateful for access to the University of Nottingham's Ada High Performance Computing Service.

Associated Content

Electronic supplementary information (ESI) available. Crystallographic data is available through the CCDC, deposit numbers: 2372409–2372413. For ESI see DOI: XXXXXX. A data repository containing computational output files and spectroscopic data in their raw (NMR) and processed forms (IR, mass spectrometry, CHN) can be found via the following DOI: http://doi.org/10.17639/nott.7443

Conflicts of interest

There are no conflicts to declare.

References

(1) Noor, A. Recent Developments in Two Coordinate Transition Metal Chemistry. *Coord. Chem. Rev.* **2023**, *476*, 214941. https://doi.org/10.1016/j.ccr.2022.214941.

(2) Kays, D. L. Extremely Bulky Amide Ligands in Main Group Chemistry. *Chem. Soc. Rev.* **2016**, *45* (4), 1004–1018. https://doi.org/10.1039/C5CS00513B.

(3) Taylor, L. J.; Kays, D. L. Low-Coordinate First-Row Transition Metal Complexes in Catalysis and Small Molecule Activation. *Dalton Trans.* **2019**, *48* (33), 12365–12381. https://doi.org/10.1039/C9DT02402F.

(4) Power, P. P. Some Highlights from the Development and Use of Bulky Monodentate Ligands. *J. Organomet. Chem.* **2004**, *689* (24), 3904–3919. https://doi.org/10.1016/j.jorganchem.2004.06.010.

(5) Mills, D. P.; Evans, P. F-Block Phospholyl and Arsolyl Chemistry. *Chem. Eur. J.* **2021**, *27* (22), 6645–6665. https://doi.org/10.1002/chem.202005231.

(6) Shan, C.; Yao, S.; Driess, M. Where Silylene–Silicon Centres Matter in the Activation of Small Molecules. *Chem. Soc. Rev.* **2020**, *49* (18), 6733–6754. https://doi.org/10.1039/D0CS00815J.

(7) Webster, R. L. β-Diketiminate Complexes of the First Row Transition Metals: Applications in Catalysis. *Dalton Trans.* **2017**, *46* (14), 4483–4498. https://doi.org/10.1039/C7DT00319F.

(8) Lipschutz, M. I.; Chantarojsiri, T.; Dong, Y.; Tilley, T. D. Synthesis, Characterization, and Alkyne Trimerization Catalysis of a Heteroleptic Two-Coordinate FeI Complex. *J. Am. Chem. Soc.* **2015**, *137* (19), 6366–6372. https://doi.org/10.1021/jacs.5b02504.

(9) Ung, G.; Rittle, J.; Soleilhavoup, M.; Bertrand, G.; Peters, J. C. Two-Coordinate Fe0 and Co0 Complexes Supported by Cyclic (Alkyl)(Amino)Carbenes. *Angew. Chem. Int. Ed.* **2014**, *53* (32), 8427–8431. https://doi.org/10.1002/anie.201404078.

(10) Zimmermann, P.; Limberg, C. Activation of Small Molecules at Nickel(I) Moieties. *J. Am. Chem. Soc.* **2017**, *139* (12), 4233–4242. https://doi.org/10.1021/jacs.6b12434.

(11) Roy, L.; Al-Afyouni, M. H.; DeRosha, D. E.; Mondal, B.; DiMucci, I. M.; Lancaster, K. M.; Shearer, J.; Bill, E.; Brennessel, W. W.; Neese, F.; Ye, S.; Holland, P. L. Reduction of CO2 by a Masked Two-Coordinate Cobalt(I) Complex and Characterization of a Proposed Oxodicobalt(II) Intermediate. *Chem. Sci.* **2019**, *10* (3), 918–929. https://doi.org/10.1039/C8SC02599A.

(12) Lei, H.; Ellis, B. D.; Ni, C.; Grandjean, F.; Long, G. J.; Power, P. P. An Arene-Stabilized Cobalt(I) Aryl: Reactions with CO and NO. *Inorg. Chem.* **2008**, *47* (22), 10205–10207. https://doi.org/10.1021/ic8015782.

(13) Sharpe, H. R.; Geer, A. M.; Taylor, L. J.; Gridley, B. M.; Blundell, T. J.; Blake, A. J.; Davies, E. S.; Lewis, W.; McMaster, J.; Robinson, D.; Kays, D. L. Selective Reduction and Homologation of Carbon Monoxide by Organometallic Iron Complexes. *Nat. Commun.* **2018**, *9* (1), 3757. https://doi.org/10.1038/s41467-018-06242-w.

(14) Lipschutz, M. I.; Tilley, T. D. Carbon–Carbon Cross-Coupling Reactions Catalyzed by a Two-Coordinate Nickel(II)–Bis(Amido) Complex via Observable NiI, NiII, and NiIII Intermediates. *Angew. Chem. Int. Ed.* **2014**, *53* (28), 7290–7294. https://doi.org/10.1002/anie.201404577.

(15) Sharpe, H. R.; Geer, A. M.; Lewis, W.; Blake, A. J.; Kays, D. L. Iron(II)-Catalyzed Hydrophosphination of Isocyanates. *Angew. Chem. Int. Ed.* **2017**, *56* (17), 4845–4848. https://doi.org/10.1002/anie.201701051.

(16) McClain, K. R.; Gould, C. A.; Chakarawet, K.; Teat, S. J.; Groshens, T. J.; Long, J. R.; Harvey, B. G. High-Temperature Magnetic Blocking and Magneto-Structural Correlations in a Series of Dysprosium(III) Metallocenium Single-Molecule Magnets. *Chem. Sci.* **2018**, *9* (45), 8492–8503. https://doi.org/10.1039/C8SC03907K.

(17) Guo, F.-S.; Day, B. M.; Chen, Y.-C.; Tong, M.-L.; Mansikkamäki, A.; Layfield, R. A. Magnetic Hysteresis up to 80 Kelvin in a Dysprosium Metallocene Single-Molecule Magnet. *Science* **2018**, *362* (6421), 1400–1403. https://doi.org/10.1126/science.aav0652.

(18) Parmar, V. S.; Mills, D. P.; Winpenny, R. E. P. Mononuclear Dysprosium Alkoxide and Aryloxide Single-Molecule Magnets. *Chem. Eur. J.* **2021**, *27* (28), 7625–7645. https://doi.org/10.1002/chem.202100085.

(19) Gould, C. A.; McClain, K. R.; Reta, D.; Kragskow, J. G. C.; Marchiori, D. A.; Lachman, E.; Choi, E.-S.; Analytis, J. G.; Britt, R. D.; Chilton, N. F.; Harvey, B. G.; Long, J. R. Ultrahard

Magnetism from Mixed-Valence Dilanthanide Complexes with Metal-Metal Bonding. *Science* **2022**, *375* (6577), 198–202. https://doi.org/10.1126/science.abl5470.

(20) Castellanos, E.; Benner, F.; Demir, S. Linear, Electron-Rich Erbium Single-Molecule Magnet with Dibenzocyclooctatetraene Ligands. *Inorg. Chem.* **2024**, *63* (21), 9888–9898. https://doi.org/10.1021/acs.inorgchem.4c00731.

(21) Bunting, P. C.; Atanasov, M.; Damgaard-Møller, E.; Perfetti, M.; Crassee, I.; Orlita, M.; Overgaard, J.; van Slageren, J.; Neese, F.; Long, J. R. A Linear Cobalt(II) Complex with Maximal Orbital Angular Momentum from a Non-Aufbau Ground State. *Science* **2018**, *362* (6421), eaat7319. https://doi.org/10.1126/science.aat7319.

(22) Zadrozny, J. M.; Xiao, D. J.; Atanasov, M.; Long, G. J.; Grandjean, F.; Neese, F.; Long, J. R. Magnetic Blocking in a Linear Iron(I) Complex. *Nat. Chem.* **2013**, *5* (7), 577–581. https://doi.org/10.1038/nchem.1630.

(23) Zadrozny, J. M.; Atanasov, M.; Bryan, A. M.; Lin, C.-Y.; Rekken, B. D.; Power, P. P.; Neese, F.; Long, J. R. Slow Magnetization Dynamics in a Series of Two-Coordinate Iron(II) Complexes. *Chem. Sci.* **2012**, *4* (1), 125–138. https://doi.org/10.1039/C2SC20801F.

(24) Yao, X.-N.; Du, J.-Z.; Zhang, Y.-Q.; Leng, X.-B.; Yang, M.-W.; Jiang, S.-D.; Wang, Z.-X.; Ouyang, Z.-W.; Deng, L.; Wang, B.-W.; Gao, S. Two-Coordinate Co(II) Imido Complexes as Outstanding Single-Molecule Magnets. *J. Am. Chem. Soc.* **2017**, *139* (1), 373–380. https://doi.org/10.1021/jacs.6b11043.

(25) Valentine, A. J.; Geer, A. M.; Blundell, T. J.; Tovey, W.; Cliffe, M. J.; Davies, E. S.; Argent, S. P.; Lewis, W.; McMaster, J.; Taylor, L. J.; Reta, D.; Kays, D. L. Slow Magnetic Relaxation in Fe(II) m-Terphenyl Complexes. *Dalton Trans.* **2022**, *51* (47), 18118–18126. https://doi.org/10.1039/D2DT03531F.

(26) Bürger, H.; Wannagat, U. Silylamido-Derivate von Eisen und Kobalt. *Monatsh. Chem.* **1963**, *94* (6), 1007–1012. https://doi.org/10.1007/BF00905688.

(27) Bürger, H.; Wannagat, U. Silylamido-Verbindungen von Chrom, Mangan, Nickel und Kupfer. *Monatsh. Chem.* **1964**, *95* (4), 1099–1102. https://doi.org/10.1007/BF00904702.

(28) Bürger, H.; Sawodny, W.; Wannagat, U. Darstellung Und Schwinkungsspektren von Silylamiden Der Elemente Zink, Cadmium Und Quecksilber. *J. Organomet. Chem.* **1965**, *3* (2), 113–120. https://doi.org/10.1016/S0022-328X(00)84740-3.

(29) Waezsada, S. D.; Belgardt, T.; Noltemeyer, M.; Roesky, H. W. [2,6-iPr2C6H3(Me3Si)NTl]4—A Covalent Thallium(I)-Nitrogen Compound with Weak Arene–Thallium Interactions. *Angew. Chem. Int. Ed.* **1994**, *33* (13), 1351–1352. https://doi.org/10.1002/anie.199413511.

(30) Petrie, M. A.; Ruhlandt-Senge, K.; Power, P. P. Synthesis and Characterization of the Monomeric Aluminum Monoamides (Tert-Bu) 2AlN(R)R’ (R and R’ = Bulky Aryl, Alkyl, or Silyl Groups). *Inorg. Chem.* **1993**, *32* (7), 1135–1141. https://doi.org/10.1021/ic00059a019.

(31) Wraage, K.; Lameyer, L.; Stalke, D.; Roesky, H. W. Reaction of RGeBr3 (R=iPr2C6H3NSiMe3) with Ammonia To Give (RGe)2(NH2)4(NH): A Compound Containing Terminal NH2 Groups. *Angew. Chem. Int. Ed.* **1999**, *38* (4), 522–523. https://doi.org/10.1002/(SICI)1521-3773(19990215)38:4<522::AID-ANIE522>3.0.CO;2-N.

(32) Babcock, J. R.; Liable-Sands, L.; Rheingold, A. L.; Sita, L. R. Syntheses, Structural Characterizations, and Heterocumulene Metathesis Studies of New Monomeric Bis(Triorganosilylamido)Tin(II) Derivatives. *Organometallics* **1999**, *18* (21), 4437–4441. https://doi.org/10.1021/om990526w.

(33) Brynda, M.; Herber, R.; Hitchcock, P. B.; Lappert, M. F.; Nowik, I.; Power, P. P.; Protchenko, A. V.; Růžička, A.; Steiner, J. Higher-Nuclearity Group 14 Metalloid Clusters: [Sn9Sn(NRR′)6]. *Angew. Chem.* **2006**, *118* (26), 4439–4443. https://doi.org/10.1002/ange.200600292.

(34) Lipschutz, M. I.; Tilley, T. D. Synthesis and Reactivity of a Conveniently Prepared Two-Coordinate Bis(Amido) Nickel(II) Complex. *Chem. Commun.* **2012**, *48* (57), 7146–7148. https://doi.org/10.1039/C2CC32974C.

(35) Lin, C.-Y.; Guo, J.-D.; Fettinger, J. C.; Nagase, S.; Grandjean, F.; Long, G. J.; Chilton, N. F.; Power, P. P. Dispersion Force Stabilized Two-Coordinate Transition Metal–Amido Complexes of the −N(SiMe3)Dipp (Dipp = C6H3-2,6-Pri2) Ligand: Structural, Spectroscopic, Magnetic, and Computational Studies. *Inorg. Chem.* **2013**, *52* (23), 13584–13593. https://doi.org/10.1021/ic402105m.

(36) Goodwin, C. A. P.; Chilton, N. F.; Vettese, G. F.; Moreno Pineda, E.; Crowe, I. F.; Ziller, J. W.; Winpenny, R. E. P.; Evans, W. J.; Mills, D. P. Physicochemical Properties of Near-Linear Lanthanide(II) Bis(Silylamide) Complexes (Ln = Sm, Eu, Tm, Yb). *Inorg. Chem.* **2016**, *55* (20), 10057–10067. https://doi.org/10.1021/acs.inorgchem.6b00808.

(37) Chilton, N. F.; Goodwin, C. A. P.; Mills, D. P.; Winpenny, R. E. P. The First Near-Linear Bis(Amide) f-Block Complex: A Blueprint for a High Temperature Single Molecule Magnet. *Chem. Commun.* **2014**, *51* (1), 101–103. https://doi.org/10.1039/C4CC08312A.

(38) Goodwin, C. A. P.; Chilton, N. F.; Natrajan, L. S.; Boulon, M.-E.; Ziller, J. W.; Evans, W. J.; Mills, D. P. Investigation into the Effects of a Trigonal-Planar Ligand Field on the Electronic Properties of Lanthanide(II) Tris(Silylamide) Complexes (Ln = Sm, Eu, Tm, Yb). *Inorg. Chem.* **2017**, *56* (10), 5959–5970. https://doi.org/10.1021/acs.inorgchem.7b00664.

(39) Thum, K.; Martin, J.; Elsen, H.; Eyselein, J.; Stiegler, L.; Langer, J.; Harder, S. Lewis Acidic Cationic Strontium and Barium Complexes. *Eur. J. Inorg. Chem.* **2021**, *2021* (26), 2643–2653. https://doi.org/10.1002/ejic.202100345.

(40) Knüpfer, C.; Klerner, L.; Mai, J.; Langer, J.; Harder, S. S-Block Metal Complexes of Superbulky (tBu3Si)2N−: A New Weakly Coordinating Anion? *Chem. Sci.* **2024**, *15* (12), 4386–4395. https://doi.org/10.1039/D3SC06896J.

(41) Goel, S. C.; Chiang, M. Y.; Buhro, W. E. Synthesis of Homoleptic Silylphosphido Complexes (M[P(SiMe3)2][.Mu.-P(SiMe3)2])2, Where M = Zinc and Cadmium, and Their Use in Metalloorganic Routes to Cd3P2 and MGeP2. *J. Am. Chem. Soc.* **1990**, *112* (14), 5636–5637. https://doi.org/10.1021/ja00170a036.

(42) Goel, S. C.; Chiang, M. Y.; Rauscher, D. J.; Buhro, W. E. Comparing the Properties of Homologous Phosphido and Amido Complexes: Synthesis and Characterization of the Disilylphosphido Complexes {M[P(SiMe3)2]2}2 Where M = Zinc, Cadmium, Mercury, Tin, Lead and Manganese. *J. Am. Chem. Soc.* **1993**, *115* (1), 160–169. https://doi.org/10.1021/ja00054a022.

(43) Englich, U.; Hassler, K.; Ruhlandt-Senge, K.; Uhlig, F. A Convenient Synthetic Strategy toward Heavy Alkali Metal Bis(Trimethylsilyl)Phosphides: Crystal Structures of the Ladder-Type Polymers [A(Thf)P(SiMe3)2]∞ (A = K, Rb, Cs). *Inorg. Chem.* **1998**, *37* (14), 3532–3537. https://doi.org/10.1021/ic9801950.

(44) Matchett, M. A.; Chiang, M. Y.; Buhro, W. E. Disilylphosphido Complexes M[P(SiPh3)2]2, Where M = Zn, Cd, Hg, and Sn: Effective Steric Equivalency of P(SiPh3)2 and N(SiMe3)2 Ligands. *Inorg. Chem.* **1994**, *33* (6), 1109–1114. https://doi.org/10.1021/ic00084a023.

(45) Schäfer, H.; Fritz, G.; Hölderich, W. Das LiPH2 ·1 Monoglym. *Z. Anorg. Allg. Chem.* **1977**, *428* (1), 222–224. https://doi.org/10.1002/zaac.19774280127.

(46) Baudler, M.; Glinka, K.; Jones, R. A. Trilithium Heptaphosphide, Dilithium Hexadecaphosphide, and Trisodium Henicosaphosphide. In *Inorganic Syntheses*; John Wiley & Sons, Ltd, 1990; pp 227–235. https://doi.org/10.1002/9780470132586.ch45.

(47) Westerhausen, M.; Löw, R.; Schwarz, W. NMR-Spektroskopische Und Strukturelle Charakterisierung Der Tri-*Iso*-Propylsilylphosphanide Des Calciums. *J. Organomet. Chem.* **1996**, *513* (1), 213–229. https://doi.org/10.1016/0022-328X(95)05971-Q.

(47) Westerhausen, M.; Rotter, T.; Görls, H.; Birg, C.; Warchhold, M.; Nöth, H. Lithium Bis(Triisopropylsilyl)Phosphanide and Its Pentacarbonyltungsten Adduct: Synthesis and Crystal Structures of the Dimer [(Thf)Li-P(SiiPr3)2]2 and the Solvent-Separated Ion Pair [(Thf)4Li]+ [(OC)5W-P(SiiPr3)2]–. *Z. Naturforsch. B* **2005**, *60* (7), 766–770. https://doi.org/10.1515/znb-2005-0712.

(48) Hänisch, C. The Tris(Triisopropylsilyl)Pnikogenes: Synthesis and Characterisation of [E(SiiPr3)3] (E = P, As, Sb). *Z.Anorg. Allg. Chem.* **2001**, *627*, 1414–1416.

(50) Gary, D. C.; Cossairt, B. M. Role of Acid in Precursor Conversion During InP Quantum Dot Synthesis. *Chem. Mater.* **2013**, *25* (12), 2463–2469. https://doi.org/10.1021/cm401289j.

(51) Bürger, H.; Goetze, U. Die Hydrolytische Spaltung von Tris(Trimethylsilyl)Derivaten Der Elemente Phosphor, Arsen Und Antimon. *J. Organomet. Chem.* **1968**, *12* (3), 451–457. https://doi.org/10.1016/S0022-328X(00)88698-2.

(52) Connelly, N. G.; Geiger, W. E. Chemical Redox Agents for Organometallic Chemistry. *Chem. Rev.* **1996**, *96* (2), 877–910. https://doi.org/10.1021/cr940053x.

(53) Corre, G. L.; Grützmacher, H. Simple Conversion of Trisodium Phosphide, Na3P, into Silyl- and Cyanophosphides and the Structure of a Terminal Silver Phosphide. *Dalton Trans.* **2022**, *51* (9), 3497–3501. https://doi.org/10.1039/D1DT04223H.

(54) Jupp, A. R.; Goicoechea, J. M. The 2-Phosphaethynolate Anion: A Convenient Synthesis and [2+2] Cycloaddition Chemistry. *Angew. Chem. Int. Ed.* **2013**, *52* (38), 10064–10067. https://doi.org/10.1002/anie.201305235.

(55) Kamer, P. C. J.; van Leeuwen, P. W. N. M. *Phosphorus(III)Ligands in Homogeneous Catalysis: Design and Synthesis*; John Wiley & Sons, Incorporated: Newark, UNITED KINGDOM, 2012.

(56) Westerhausen, M.; Rotter, T.; Görls, H.; Birg, C.; Warchhold, M.; Nöth, H. Lithium Bis(Triisopropylsilyl)Phosphanide and Its Pentacarbonyltungsten Adduct: Synthesis and Crystal Structures of the Dimer [(Thf)Li-P(SiiPr3)2]2 and the Solvent-Separated Ion Pair [(Thf)4Li]+ [(OC)5W-P(SiiPr3)2]–. *Zeitschrift für Naturforschung B* **2005**, *60* (7), 766–770. https://doi.org/10.1515/znb-2005-0712.

(57) Baldwin, J.; Brookfield, A.; Whitehead, G. F. S.; Natrajan, L. S.; McInnes, E. J. L.; Oakley, M. S.; Mills, D. P. Synthesis and Characterization of Solvated Lanthanide (II) Bis(Triisopropylsilyl)Phosphide Complexes. *Personal Communication*.

(58) Nesterov, V.; Breit, N. C.; Inoue, S. Advances in Phosphasilene Chemistry. *Chem. Eur. J.* **2017**, *23* (50), 12014–12039. https://doi.org/10.1002/chem.201700829.

(59) King, R. B. Atomic Orbitals, Symmetry, and Coordination Polyhedra. *Coord. Chem. Rev* **2000**, *197* (1), 141–168. https://doi.org/10.1016/S0010-8545(99)00226-X.

(60) C. Cole, S.; P. Coles, M.; B. Hitchcock, P. Dimesitylzinc : A Strictly 2-Coordinate, Homoleptic Diarylzinc Compound. *Dalton Trans.* **2003**, *0* (19), 3663–3664. https://doi.org/10.1039/B309709A.

(61) Fox, B. S.; Beyer, M. K.; Bondybey, V. E. Coordination Chemistry of Silver Cations. *J. Am. Chem. Soc.* **2002**, *124* (45), 13613–13623. https://doi.org/10.1021/ja0176604.

(62) Margraf, G.; Lerner, H.-W.; Bolte, M.; Wagner, M. Kristallstruktur Des Zinkamids Zn[N(SiMe3)2]2. *Z. Anorg. Allg. Chem.* **2004**, *630* (2), 217–218. https://doi.org/10.1002/zaac.200300293.

(63) Chisholm, M. H.; Gallucci, J. C.; Yin, H.; Zhen, H. Arylzinc Alkoxides: [ArZnOCHP]2 and Ar2Zn3(OCHP)4 When Ar = C6H5, p-CF3C6H4, 2,4,6-Me3C6H2, and C6F5. *Inorg. Chem.* **2005**, *44* (13), 4777–4785. https://doi.org/10.1021/ic048332i.

(64) Schröder, A.; Lork, E.; Beckmann, J. Synthesis and Structure of Bis(m-Terphenyl)Zinc (2,6-Mes2 C6 H3)2 Zn. *Main Group Met. Chem.* **2014**, *37* (5–6), 155–157. https://doi.org/10.1515/mgmc-2014-0021.

(65) Wolters, L. P.; Bickelhaupt, F. M. Nonlinear D10-ML2 Transition-Metal Complexes. *ChemistryOpen* **2013**, *2* (3), 106–114. https://doi.org/10.1002/open.201300009.

(66) Blundell, T. J.; Hastings, F. R.; Gridley, B. M.; Moxey, G. J.; Lewis, W.; Blake, A. J.; Kays, D. L. Ligand Influences on Homoleptic Group 12 M-Terphenyl Complexes. *Dalton Trans.* **2014**, *43* (38), 14257–14264. https://doi.org/10.1039/C4DT00647J.

(67) Krieck, S.; Görls, H.; Westerhausen, M. Bis(2,4,6-Trimethyl-phen-yl)Zinc(II). *Acta Cryst E* **2009**, *65* (7), m809–m809. https://doi.org/10.1107/S1600536809023186.

(68) Valentine, A. J.; Taylor, L. J.; Geer, A. M.; Huke, C. D.; Wood, K. E.; Tovey, W.; Lewis, W.; Argent, S. P.; Teale, A. M.; McMaster, J.; Kays, D. L. Structural and Electronic Studies of Substituted M-Terphenyl Group 12 Complexes. *Organometallics* **2022**, *41* (11), 1426–1433. https://doi.org/10.1021/acs.organomet.2c00156.

(65) Gridley, B. M.; Moxey, G. J.; Lewis, W.; Blake, A. J.; Kays, D. L. Conformational Isomerism in Monomeric, Low-Coordinate Group 12 Complexes Stabilized by a Naphthyl-Substituted m-Terphenyl Ligand. *Chem. Eur. J.* **2013**, *19* (34), 11446–11453. https://doi.org/10.1002/chem.201301872.

(66) Westerhausen, M.; Oßberger, M. W.; Alexander, J. S.; Ruhlandt-Senge, K. Influence of the Steric Demand of the 2,4,6-Trialkylphenyl Substituents on the Structures and Reactivity of Diarylzinc. *Z. Anorg. Allg. Chem.* **2005**, *631* (13–14), 2836–2841. https://doi.org/10.1002/zaac.200500165.

(71) Brooker, S.; Bertel, N.; Stalke, D.; Noltemeyer, M.; Roesky, H. W.; Sheldrick, G. M.; Edelmann, F. T. Main-Group Chemistry of the 2,4,6-Tris(Trifluoromethyl)Phenyl Substituent: X-Ray Crystal Structures of [2,4,6-(CF3)3C6H2]2Zn, [2,4,6-(CF3)3C6H2]2Cd(MeCN) and [2,4,6-

(CF3)3C6H3]2Hg. *Organometallics* **1992**, *11* (1), 192–195. https://doi.org/10.1021/om00037a037.
(72) Perdew, J. P.; Burke, K.; Ernzerhof, M. Generalized Gradient Approximation Made Simple. *Phys. Rev. Lett.* **1996**, *77* (18), 3865–3868. https://doi.org/10.1103/PhysRevLett.77.3865.
(66) Adamo, C.; Barone, V. Toward Reliable Density Functional Methods without Adjustable Parameters: The PBE0 Model. *J. Chem. Phys.* **1999**, *110* (13), 6158–6170. https://doi.org/10.1063/1.478522.
(67) van Lenthe, E.; Snijders, J. G.; Baerends, E. J. The Zero-order Regular Approximation for Relativistic Effects: The Effect of Spin–Orbit Coupling in Closed Shell Molecules. *J. Chem. Phys.* **1996**, *105* (15), 6505–6516. https://doi.org/10.1063/1.472460.
(68) Weigend, F.; Furche, F.; Ahlrichs, R. Gaussian Basis Sets of Quadruple Zeta Valence Quality for Atoms H–Kr. *J. Chem. Phys.* **2003**, *119* (24), 12753–12762. https://doi.org/10.1063/1.1627293.
(69) Schäfer, A.; Horn, H.; Ahlrichs, R. Fully Optimized Contracted Gaussian Basis Sets for Atoms Li to Kr. *J. Chem. Phys.* **1992**, *97* (4), 2571–2577. https://doi.org/10.1063/1.463096.
(70) Schäfer, A.; Huber, C.; Ahlrichs, R. Fully Optimized Contracted Gaussian Basis Sets of Triple Zeta Valence Quality for Atoms Li to Kr. *J. Chem. Phys.* **1994**, *100* (8), 5829–5835. https://doi.org/10.1063/1.467146.
(78) Weigend, F.; Ahlrichs, R. Balanced Basis Sets of Split Valence, Triple Zeta Valence and Quadruple Zeta Valence Quality for H to Rn: Design and Assessment of Accuracy. *Phys. Chem. Chem. Phys.* **2005**, *7* (18), 3297–3305. https://doi.org/10.1039/B508541A.
(72) Pantazis, D. A.; Chen, X.-Y.; Landis, C. R.; Neese, F. All-Electron Scalar Relativistic Basis Sets for Third-Row Transition Metal Atoms. *J. Chem. Theory Comput.* **2008**, *4* (6), 908–919. https://doi.org/10.1021/ct800047t.
(80) Pidcock, A. Coupling and “Virtual” Coupling in the Nuclear Magnetic Resonance Spectra of Phosphine Complexes. *Chem. Commun. (London)* **1968**, No. 2, 92–92. https://doi.org/10.1039/C19680000092.
(81) Hersh, W. H. False AA’X Spin-Spin Coupling Systems in 13C NMR: Examples Involving Phosphorus and a 20-Year-Old Mystery in Off-Resonance Decoupling. *J. Chem. Educ.* **1997**, *74* (12), 1485. https://doi.org/10.1021/ed074p1485.
(82) Verstuyft, A. W.; Nelson, J. H.; Cary, L. W. Investigation of the Utility of “Virtual Coupling” in the 13C{1H) Nuclear Magnetic Resonance Spectra of Bis-Phosphite Complexes of Palladium and Platinum. Algebraic Cancelation of Spin-Spin Coupling. *Inorg. Chem.* **1975**, *15* (3), 732–734.